

RESEARCH

Open Access



Global patterns of rebound to normal RSV dynamics following COVID-19 suppression

Deus Thindwa^{1*}, Ke Li¹, Dominic Cooper-Wootton¹, Zhe Zheng¹, Virginia E Pitzer¹ and Daniel M Weinberger^{1*}

Abstract

Background Annual epidemics of respiratory syncytial virus (RSV) had consistent timing and intensity between seasons prior to the SARS-CoV-2 pandemic (COVID-19). However, starting in April 2020, RSV seasonal activity declined due to COVID-19 non-pharmaceutical interventions (NPIs) before re-emerging after relaxation of NPIs. We described the unusual patterns of RSV epidemics that occurred in multiple subsequent waves following COVID-19 in different countries and explored factors associated with these patterns.

Methods Weekly cases of RSV from twenty-eight countries were obtained from the World Health Organisation and combined with data on country-level characteristics and the stringency of the COVID-19 response. Dynamic time warping and regression were used to cluster time series patterns and describe epidemic characteristics before and after COVID-19 pandemic, and identify related factors.

Results While the first wave of RSV epidemics following pandemic suppression exhibited unusual patterns, the second and third waves more closely resembled typical RSV patterns in many countries. Post-pandemic RSV patterns differed in their intensity and/or timing, with several broad patterns across the countries. The onset and peak timings of the first and second waves of RSV epidemics following COVID-19 suppression were earlier in the Southern than Northern Hemisphere. The second wave of RSV epidemics was also earlier with higher population density, and delayed if the intensity of the first wave was higher. More stringent NPIs were associated with lower RSV growth rate and intensity and a shorter gap between the first and second waves.

Conclusion Patterns of RSV activity have largely returned to normal following successive waves in the post-pandemic era. Onset and peak timings of future epidemics following disruption of normal RSV dynamics need close monitoring to inform the delivery of preventive and control measures.

Keywords Respiratory syncytial virus, Epidemic onset, Epidemic peak, Epidemic rebound, Dynamic time warping

*Correspondence:

Deus Thindwa
deus.thindwa@yale.edu
Daniel M Weinberger
daniel.weinberger@yale.edu

¹Department of Epidemiology of Microbial Diseases and the Public Health Modeling Unit, Yale School of Public Health, New Haven, CT, USA



© The Author(s) 2024. **Open Access** This article is licensed under a Creative Commons Attribution 4.0 International License, which permits use, sharing, adaptation, distribution and reproduction in any medium or format, as long as you give appropriate credit to the original author(s) and the source, provide a link to the Creative Commons licence, and indicate if changes were made. The images or other third party material in this article are included in the article's Creative Commons licence, unless indicated otherwise in a credit line to the material. If material is not included in the article's Creative Commons licence and your intended use is not permitted by statutory regulation or exceeds the permitted use, you will need to obtain permission directly from the copyright holder. To view a copy of this licence, visit <http://creativecommons.org/licenses/by/4.0/>. The Creative Commons Public Domain Dedication waiver (<http://creativecommons.org/publicdomain/zero/1.0/>) applies to the data made available in this article, unless otherwise stated in a credit line to the data.

Background

Respiratory syncytial virus (RSV) causes a high burden of respiratory disease among infants and older adults [1–3] and is an important cause of death in the first year of life [1]. RSV spreads through contact with infectious droplets, and transmission is strongly seasonal, with annual epidemics in most regions typically occurring during the autumn or winter seasons [4, 5]. Understanding temporal variations in healthcare utilization due to RSV is vital to inform planning of hospital capacity, administration of immunoprophylaxis, timing of vaccination, and enrollment for clinical trials of RSV prevention and treatment [6].

Prior to the pandemic caused by SARS-CoV-2 (COVID-19), annual epidemics of RSV largely followed consistent temporal patterns year-to-year in each country [7]. However, during the COVID-19 pandemic, RSV seasonal activity decreased to very low levels starting in March 2020 [8–13]. This was likely due to implementation of non-pharmaceutical interventions (NPIs) such as country-wide lockdowns, border closures, social distancing, face masks, and school closures that were intended to contain the spread of SARS-CoV-2 [8, 14, 15]. After the early phase of the COVID-19 pandemic and the easing of some NPIs [16], RSV activity was heterogeneous across countries, with some countries reporting a rapid return of RSV and others experiencing delayed epidemics. The characteristics of these resurgent epidemics were unexpected and included out-of-season epidemics, a high volume of cases, and multiple within-country outbreaks [17–20]. These unusual patterns highlighted the current and future need to better understand RSV epidemic patterns.

A number of factors were associated with the timing of the initial rebound in RSV activity following COVID-19 suppression [15, 21]. Reopening of schools, increasing population susceptibility or “immunity debt”, and decreasing temperatures were reported to increase the risk of initial RSV rebound [14, 15, 21]. However, as predicted by modeling studies during the initial period of disruption [22], it could take several seasons to return to pre-pandemic seasonal patterns of RSV activity (“return to normal”). The determinants of the return to normal are not fully understood.

In this study, we collated epidemiologic, demographic, climate, geography, and behavioral data from twenty-eight countries globally, from 2017 to 2023. We used these data to measure the correlation of RSV patterns between pre- and post-COVID-19 pandemic period, identify distinct patterns of RSV related to onset, peak timing, growth rate and intensity, and explore their associated factors following RSV disruptions related to COVID-19.

Methods

Data description

We obtained publicly available data on weekly counts of RSV cases by country and hemisphere from January 2017 to July 2023 from the World Health Organisation (WHO) FluNet platform [7, 23], which is a web-based tool for influenza and RSV virological surveillance ([https://frontdoor-l4uikgap6gz3m.azurefd.net/FLUMART/VIW_FNT?\\$format=csv](https://frontdoor-l4uikgap6gz3m.azurefd.net/FLUMART/VIW_FNT?$format=csv)) [7]. We included countries which met the criteria of reporting at least 100 annual RSV cases between 2017 and 2023. This threshold was chosen empirically because models did not consistently converge when fit to data from countries with more sparse data. In brief, RSV data were transmitted to FluNet from each country’s recognized national influenza center or national public health laboratory with ongoing influenza surveillance and laboratory capacity for RSV testing using molecular methods and with a history of successful WHO external quality assessment for the molecular detection of influenza [7]. Additional data on a country’s climate zone were obtained from the US National Oceanic Atmospheric Administration based on Köppen and Geiger classification [24], whereas a country’s COVID-19 contact stringency index and population density were obtained from the Oxford COVID-19 Government Response Tracker [16]. Population density was calculated as the number of people per square kilometers of land area in 2020 in each country. Stringency index was calculated as a composite measure of the government’s response based on nine response indicators including school closures, workplace closures, and travel bans, rescaled to a value from 0 to 100, (100=strictest).

Statistical analyses

Generalised additive modelling

To smooth the data prior to analysis, we fitted generalised additive models (GAM) with penalized B-splines (P-splines) to weekly counts of RSV cases over the entire 312-week study period, as defined separately for the Northern and Southern hemispheres [25]. A log-linked GAM was fitted with a Poisson likelihood using maximum likelihood based on the framework that was developed for outbreak time series [26, 27]. Details of the GAM P-spline model are presented in the Supplement (Text S1).

Dynamic time warping and time series classification

We sought to cluster RSV time series based on the dynamics during the pre- and post-pandemic periods in 26 countries. To do this, we used dynamic time warping (DTW) to evaluate pairwise similarity between P-spline time series. We focused on the period from Jan-08-2017 to Dec-31-2022 in the Southern Hemisphere and from Jun-11-2017 to Jun-04-2023 in the Northern Hemisphere

[28]. DTW, as implemented in the dtwclust and dtw R packages, aligns a query (Q) and reference (R) pair of P-spline time series based on common features, and calculates distances between the two P-spline time series to form a local cost matrix (LCM), where each element (i, j) of the matrix corresponding to the Euclidean distance between Q_i and R_j [28–30]. We first normalized the P-spline time series from each country before performing the DTW. Since clustering accuracy is influenced by warping window size [31, 32], and our interest also included matching RSV dynamics in nearby seasons, we tested different warping window sizes (from 1 to 100 weeks) as well as using the entire warping window as part of a sensitivity analysis. A warping distance, which minimizes the alignment between the two P-spline time series, is computed under the constraint of Sakoe-Chiba band window size of the LCM. We selected an optimal window size from a range of values through evaluation of hierarchical clusters as detailed in the Supplement [30, 31, 33] (Fig. 1, Text S2). Hierarchical clustering was performed based on the estimated warping distances [34] and was visualized as a dendrogram. A prototype time series for each cluster summarized the most important characteristics of all series in each cluster using a DTW barycentre averaging function [30].

Description of post-pandemic epidemic patterns

Given the distinct clusters of RSV epidemics and that some epidemics in the Southern (e.g., South Africa, Australia) and Northern (e.g., United States, the Netherlands) hemispheres occurred during unusual times of the year following COVID-19 suppression, we report on metrics describing the first, second and third waves of RSV in comparison to a ‘typical season’ from the pre-COVID-19 era. ‘Epidemic years’ are defined as weeks 1–52 of the calendar year for the Southern hemisphere and weeks 24–52 and 1–23 of successive calendar years for the Northern hemisphere. The three waves were defined as separate epidemics in a given country if their onsets occurred at least eight weeks apart.

We computed four metrics to describe the dynamics of RSV activity following suppression of transmission during the initial part of the COVID-19 pandemic (starting April 1, 2020): RSV onset timing, peak timing, growth rate, and intensity. Using the fitted P-splines, we estimated the following metrics for each pre-COVID-19 season and post-COVID-19 wave [27], as detailed in the supplement (Text S3):

- Onset timing: the week when the rate of change of growth rate increased the most, corresponding to

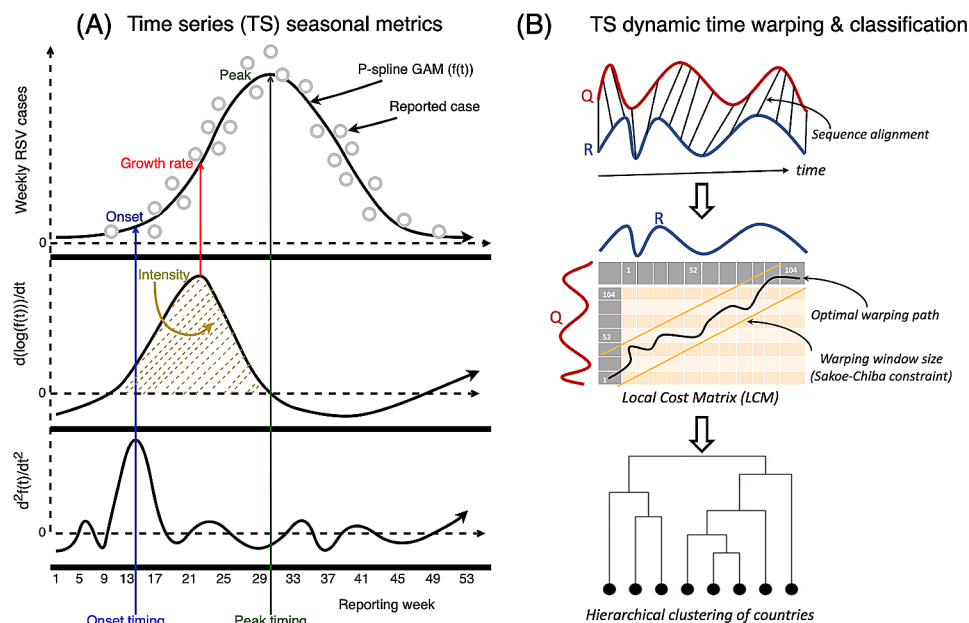


Fig. 1 Schematic diagram of respiratory syncytial virus (RSV) seasonal metrics and time series classification. **(A)** A P-spline (black line curve) is fitted to weekly RSV case counts (circles); peak timing is the week of maximum number of seasonal cases corresponding to the week when the fitted P-spline curve in each season/wave is at a maximum (A-top). The growth rate is the weekly change in new cases corresponding to the maximum value of the derivative of log fitted P-spline curve; and intensity is the relative magnitude of the epidemic peak, corresponding to the integral of positive segment of first derivative of the log fitted P-spline curve (A-middle). Onset timing is the week when the growth rate increases the most, corresponding to week when second derivative of the fitted P-spline curve is at a maximum (A-bottom); **(B)** Dynamic time warping (DTW) of RSV time series (TS); the time series of any two countries are realigned to measure their dissimilarity (B-top), based on optimal warping distance from a local cost matrix (B-middle), resulting in a hierarchical clustering of countries (B-bottom). Created with Draw.io software [45]

the time point when the second derivative of the P-spline curve was at the maximum value during the period when the growth rate (first derivative) was increasing in each season or wave (Figure S1) [18]. Unlike other definitions, our approach does not rely on having full epidemic data and some percentage threshold to determine outbreak onset. Other definitions can be particularly sensitive to changes in testing over time, which was a particular concern in the post-pandemic period.

- b. Peak timing: the week with the highest number of cases in each season or wave, corresponding to the highest points of the fitted P-spline curve (Figure S2).
- c. Growth rate: the maximum rate of change of log-transformed cases, corresponding to the maximum value of the first derivative of the log-transformed fitted P-spline curve in each season or wave (Figure S3) [35].
- d. Intensity: the relative magnitude of the epidemic peak in each season or wave, corresponding to the integral of the positive first derivative of log-transformed fitted P-spline curve. This is equivalent to the sum of the log of the fitted P-spline at the peak minus the start of the epidemic (Figure S4).

Predictors of post-pandemic patterns

For each of the four metrics described above (RSV onset timing, peak timing, growth rate, and intensity), we compared the pre-pandemic RSV seasonal patterns with those observed in the first, second and third RSV epidemic waves in various countries following COVID-19 suppression. We used Pearson's correlation coefficients to quantify relationships with RSV growth rate and intensity, and circular correlation coefficients to quantify relationships with RSV onset and peak timing, stratified by hemisphere and climate zone.

We used Cox Proportional Hazard regression to evaluate potential predictors of the time to onset or time to peak of the first epidemic wave after April 2020. We also evaluated predictors of the time between onset or peak timing of the second epidemic wave and the onset of the first wave using Cox models. We further evaluated predictors of RSV growth rate and intensity in each post-pandemic wave using linear regression. Potential predictors included hemisphere, climate zone, contact stringency index, population density, and out-of-season status and intensity during first RSV wave. All potential predictors were included in univariate analyses, and those with $p < 0.10$ were retained for multivariate analyses. Univariate predictors were included in the multivariate models through

a stepwise forward selection procedure if they reduced the Akaike Information Criterion (AIC) score [36, 37].

Results

Data description

There were 28 countries that met the inclusion criteria and were included in the analysis. Of these, 21 (75.0%) and 7 (25.0%) were from the Northern and Southern hemispheres, respectively. Thirteen (46.4%) countries had temperate climates, and 15 (53.6%) were from (sub) tropical zones, with representation from Europe ($n=12$, 42.9%), South America ($n=6$, 21.4%), North America ($n=3$, 10.7%), Western Pacific ($n=3$, 10.7%), Africa ($n=1$, 3.6%), Southeast Asia ($n=1$, 3.6%), and Eastern Mediterranean (2, 7.1%). Population density was higher in the Northern than Southern hemisphere, and in the temperate than (sub)tropical climate zones whereas contact stringency index largely declined from 2020 to 2023, with varying rates of decline between countries (Figure S5, Figure S6). While most countries were estimated to have had two RSV waves in the post-pandemic period, Australia, Brazil, Colombia, France, Iceland, the Netherlands and South Africa had three waves (Fig. 2, Figure S1, Figure S2).

Distinct epidemic clusters during the first and second RSV waves

We identified three clusters as the optimal number of clusters of the 24 possible clusters, which exhibited three general patterns of RSV activity following COVID-19 suppression (Fig. 3, Figure S7). The clusters provide a rough method for grouping countries, and not all countries within a cluster necessarily followed the average patterns: (a) cluster 1 was largely characterised by similar delayed and low-intensity patterns of the first wave relative to the pre-pandemic era for country members like Iceland, South Africa, Qatar, Argentina, Ireland, Oman, Scotland, and by earlier and high-intensity patterns for the second wave relative to the pre-pandemic era for country members like Brazil, Mexico, Northern Ireland, Mongolia, Germany, Denmark, Sweden, Netherlands, France, Portugal, Canada, Spain, and United States; (b) Australia, Costa Rica, and Japan formed cluster 2, with a high-intensity first wave followed by low-intensity second wave; and (c) Paraguay, Hungary, and Peru formed cluster 3, with a low-intensity first wave followed by a high-intensity second wave (Fig. 3).

In a sensitivity analysis, compared to the base scenario with three clusters, increasing the number of clusters to four (DTW window of size 74 weeks) only resulted in unclustering of cluster 1 into two distinct clusters, whereas reducing the number of clusters to two (DTW window of size 71 weeks) resulted in reclustering of clusters 1 and 2 together (Figure S8). The use of the entire

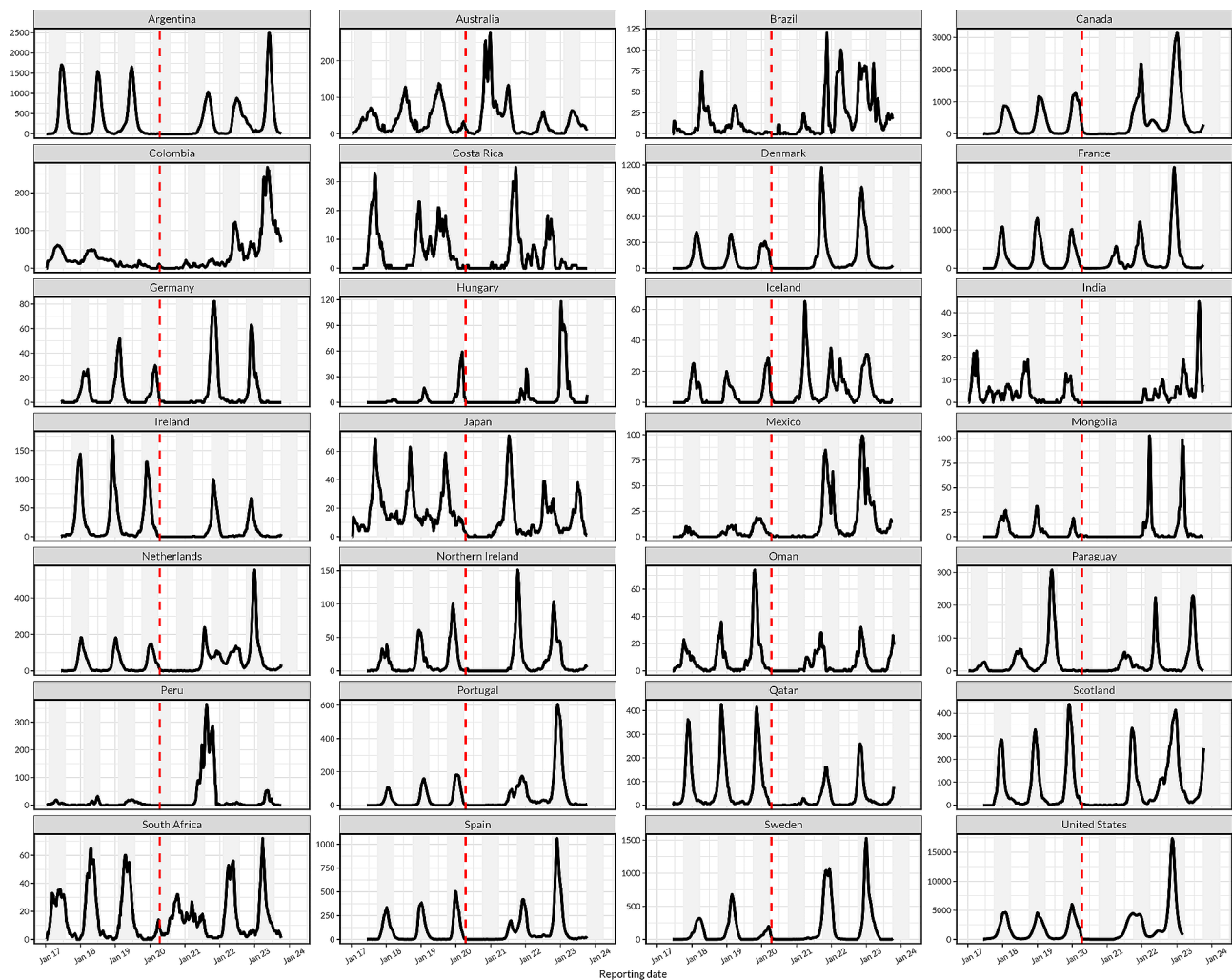


Fig. 2 Time series of respiratory syncytial virus (RSV) epidemics across 28 countries. RSV time series from 2017 to 2023 for countries in the Northern and Southern hemispheres show substantial declines in the number of reported cases following the onset of the SARS-CoV-2 pandemic (COVID-19) in 2020 when non-pharmaceutical interventions were implemented in most countries (the onset of COVID-19 is shown by a red vertical line). Heterogeneous RSV patterns are observed thereafter, including unexpected delayed onset, elevated intensity, or multiple annual outbreaks within countries when compared to the pre-COVID-19 period. The vertical shading corresponds to each country's typical RSV season, which is October to March in the Northern hemisphere and February to July in the Southern hemisphere

warping window without any constraints on window size yielded an optimal number of clusters of three, and its results were similar to the base scenario except Australia and Paraguay moved from clusters 2 and 3, respectively, to cluster 1 (Figure S9).

Epidemic patterns were more normal during the second wave

The first epidemic wave following COVID-19 generally occurred during a time of year when RSV was not typically present (Fig. 4). Epidemic onset was more than 8 weeks different from normal seasonal timing in 18 (64.3%) countries. However, in the second and third waves of RSV following COVID-19, onset timing was closer to normal across all countries (circular

correlation coefficient of $c_3 = 0.97$, $c_2 = 0.68$, $c_1 = 0.09$ in the third, second, and first waves, respectively) (Fig. 4). This was largely seen in both the Northern hemisphere ($c_3 = 0.50$, $c_2 = 0.48$, $c_1 = -0.08$) and Southern hemisphere ($c_3 = 0.75$, $c_2 = 0.05$, $c_1 = 0.17$). Similar patterns were seen when evaluating peak timing across all countries ($c_3 = 0.73$, $c_2 = 0.40$, $c_1 = 0.31$), in the Northern hemisphere ($c_3 = 0.87$, $c_2 = 0.58$, $c_1 = 0.25$) and in the Southern hemisphere ($c_3 = 0.57$, $c_2 = -0.45$, $c_1 = 0.50$) (Figure S10). Similar movement towards normal dynamics was also seen when comparing growth rates and intensity in both the Northern and Southern hemispheres (Figure S10) and across climate zones (Figure S11). Among countries with all the three waves, correlation coefficients of RSV onset timing, peak timing, growth

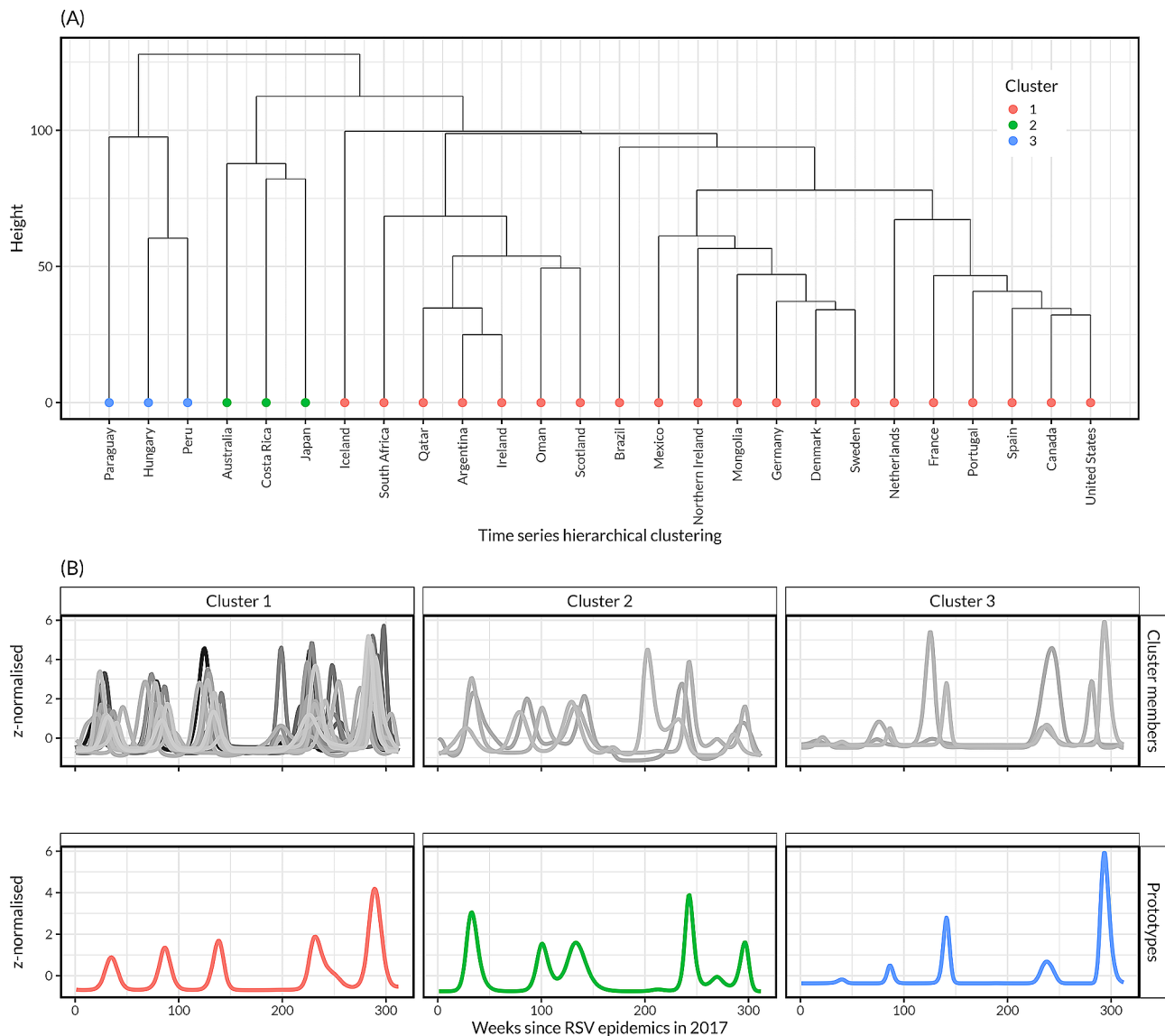


Fig. 3 Respiratory syncytial virus (RSV) time series classification of 26 countries using dynamic time-warping (DTW) and hierarchical clustering. **(A)** Hierarchical clustering of countries based on optimal DTW window size of 60 and 3 clusters, with cluster 1 having 20 countries, cluster 2 having 3 countries, and cluster 3 having 3 countries. **(B)** Cluster members and their respective prototypes (or centroids from averaging cluster members) based on DTW barycentre averaging. India and Colombia were excluded due to their unique time series

rate and intensity were also closer to pre-COVID-19 mean estimates for the third compared to the second wave (Table S1).

We observed patterns in the relationship between the onset timing and intensity of RSV epidemic waves. Generally, countries with three waves and out-of-season RSV onset (e.g. the Netherlands in the Northern hemisphere; Colombia, South Africa and Brazil in the Southern hemisphere) had large first epidemic waves followed by relatively low-intensity epidemics during the second wave. However, their second wave epidemics poorly matched their typical onset timing. On the other hand, the general pattern of countries with two waves showed that, during

the second wave, their onset timing had aligned with a typical RSV onset (Fig. 5). Irrespective of hemisphere, the mean intensity of the first wave was higher than that of the second wave, which was in turn similar to the third wave (Figure S12).

Predictors of epidemic characteristics during the first RSV wave

In univariate analysis, during the first wave following COVID-19 suppression, RSV onset and peak timing were earlier in the Southern than Northern hemisphere (hazard ratio (HR): 23.34, 95% confidence interval (CI): 7.21–75.49) and (HR: 31.42, 95% CI: 8.26–119.52), respectively,

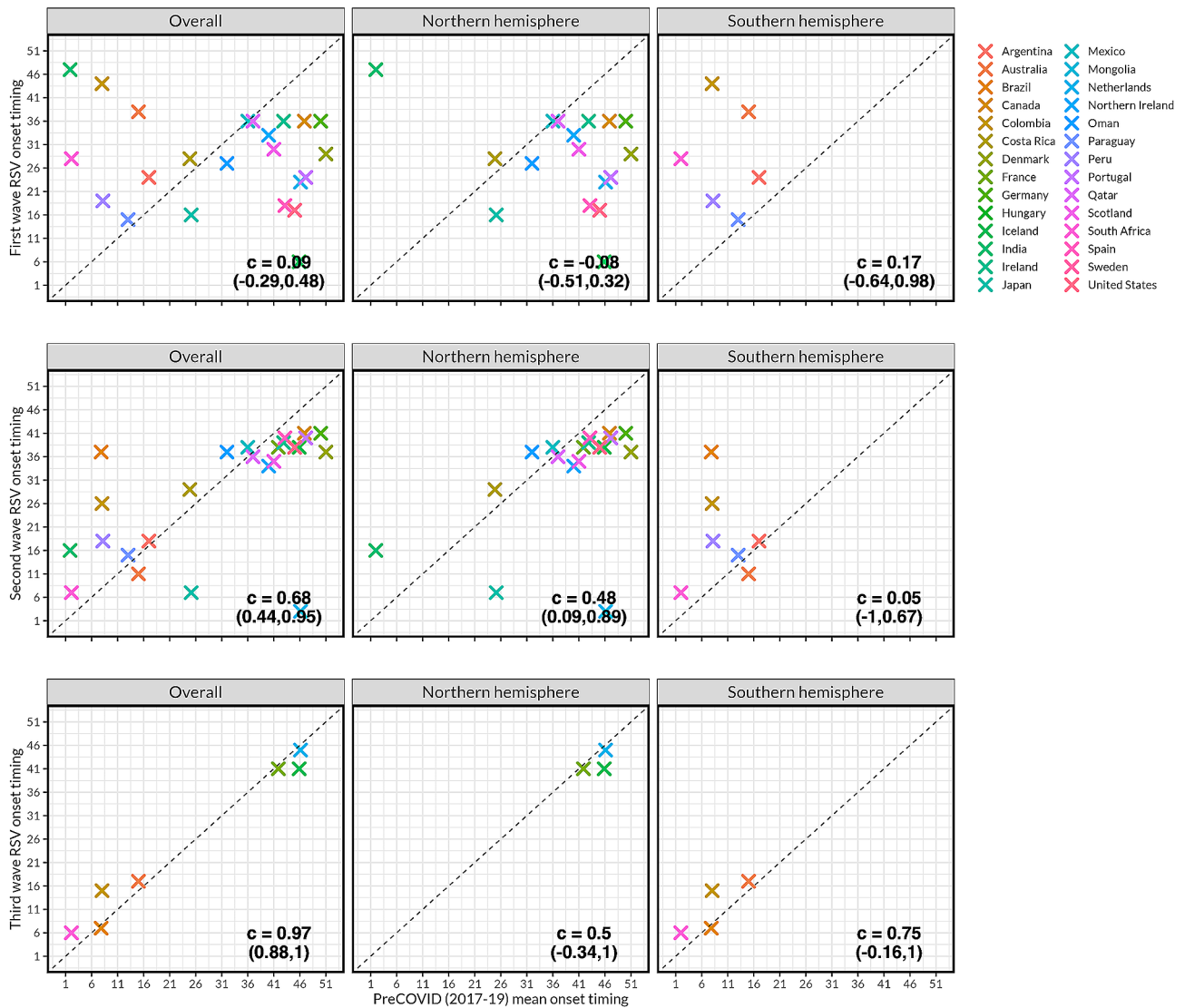


Fig. 4 Respiratory syncytial virus (RSV) epidemic onset timing during the first, second and third waves of RSV compared to mean pre-COVID-19 timing in all countries, and by Northern and Southern hemispheres. The *c* metric refers to the circular correlation coefficient; the values in parentheses correspond to the 95% confidence intervals. Overall, the plot shows that while the first wave of RSV post-COVID-19 suppression exhibited unusual patterns, the second wave and third wave more closely resembled typical RSV patterns in many countries

whereas RSV intensity was lower in tropical/subtropical than temperate areas (0.33, 95% CI: 0.11–1.02) (Table 1).

Predictors of epidemic characteristics during the second RSV wave

In multivariate analysis, the gap between the onset of the first and second waves was shorter in the Southern than Northern hemisphere (HR: 28.99, 95% CI: 4.12–203.99) and was earlier in countries with higher contact stringency (HR: 4.05, 95% CI: 1.63–10.05) and higher population density (HR: 3.89, 95% CI: 1.98–7.64). The gap between the onset of the first and second waves was longer with higher first wave intensity (HR: 0.36, 95% CI: 0.20–0.63). Peak timing of the second wave was also

earlier in the Southern than Northern hemisphere (HR: 15.39, 95% CI: 2.81–84.11), in the tropical/subtropical than temperate (HR: 2.64, 95% CI: 1.01–7.63) and with higher contact stringency (HR: 3.19, 95% CI: 1.66–6.13) (Table 2).

Discussion

We used time-series and regression analyses to understand the global RSV patterns following COVID-19 suppression. While the first post-COVID-19 wave of RSV exhibited unusual patterns, the second and third waves more closely resembled typical RSV patterns in many countries. Post-pandemic RSV patterns were broadly distinct in their intensity and timing of the onset and peak.

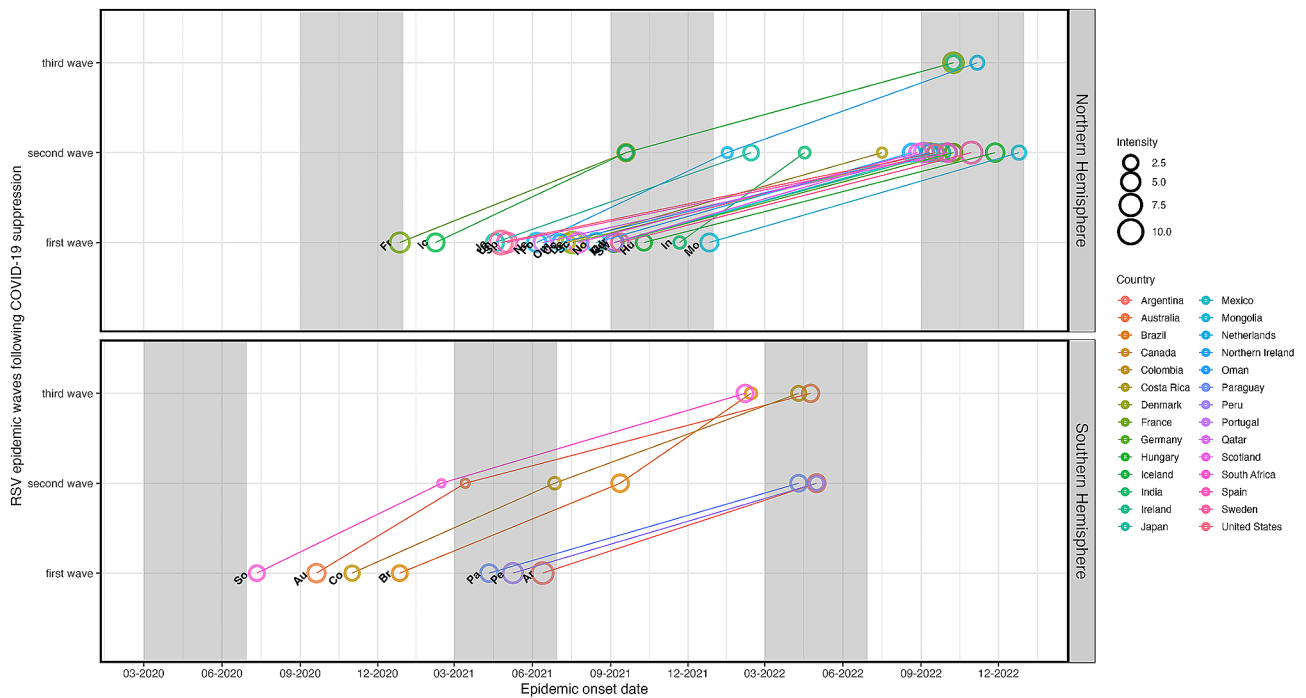


Fig. 5 Relationship between respiratory syncytial virus (RSV) epidemic onset and intensity following COVID-19 suppression in April 2020. Epidemic onset and intensity across three RSV waves stratified by hemisphere. Each circle represents a country with RSV onset date on the X-axis and RSV wave on the Y-axis; the size of the circle is proportional to intensity of RSV activity during that wave. The vertical shaded region in each hemisphere represents the onset of a typical RSV epidemic in the pre-COVID-19 period across different countries (e.g. March–June in the Southern hemisphere and September–December in the Northern hemisphere)

Table 1 Predictors of respiratory syncytial virus (RSV) onset timing, peak timing, growth rate and intensity during RSV first wave after the early phase of COVID-19 suppression in 2020 using data from 28 countries globally

Potential predictor	Univariate Cox models for onset and peak timing, and linear models for growth rate and intensity			
	Onset timing Hazard Ratio, 95%CI	Peak timing Hazard Ratio, 95%CI	Growth rate Linear Effect, 95%CI	Intensity Linear Effect, 95%CI
Hemisphere [†]				
Northern	Ref	Ref	Ref	Ref
Southern	23.34 (7.21–75.49)*	31.42 (8.26–119.52)*	1.05 (0.78–1.40)	0.69 (0.17–2.68)
Climate zone [‡]				
Temperate	Ref	Ref	Ref	Ref
(Sub)Tropical	0.70 (0.31–1.57)	0.59 (0.26–1.30)	1.09 (0.85–1.41)	0.33 (0.11–1.02)*
Contact stringency [#]	1.25 (0.84–1.87)	1.39 (0.91–2.13)	1.05 (0.93–1.20)	1.10 (0.59–2.04)
Population density ^{&}	0.88 (0.62–1.25)	0.97 (0.69–1.37)	1.01 (0.88–1.14)	0.78 (0.42–1.44)

[†] Countries in the Northern and Southern hemisphere as defined by the World Health Organisation (WHO)

[‡] Countries in the temperate, subtropical, and tropical climate zone per Köppen and Geiger classification

[#] Contact stringency index from the Oxford Coronavirus Government Response Tracker (OxCGRT)

[&] Population density per United Nations projections measured as the number of people per square kilometers of land area in 2020

[¶] Population median age per United Nations projections in 2020 in each country

* Statistical significance at $p < 0.05$, corresponding to 95% confidence intervals (95%CI)

The onset and peak timings of RSV activity following COVID-19 suppression were earlier in the Southern than Northern hemisphere for both the first and second RSV waves, whereas the intensity of first wave was lower in the tropical/subtropical than temperate countries. The gap between the onset of the first and second waves of RSV was also shorter in the countries with higher population

density, and was longer if the intensity of the first wave was higher. While higher contact stringency limited growth rate and intensity, it was associated with a shorter gap between the onset or peak of the first and second waves. Moreover, the peak timing was also earlier in the tropical/subtropical than temperate countries. Overall, our findings underscore different factors that may

Table 2 Predictors of respiratory syncytial virus (RSV) onset timing, peak timing, growth rate and intensity during the second post-COVID wave of RSV using data from 28 countries globally

Potential predictor	Univariate Cox models for onset and peak timing, and linear models for growth rate and intensity				Multivariate Cox model for onset and peak timing	
	Onset timing Hazard Ratio (95%CI)	Peak timing Hazard Ratio (95%CI)	Growth rate Linear Effect (95%CI)	Intensity Linear Effect (95%CI)	Onset timing Hazard Ratio (95%CI)	Peak timing Hazard Ratio (95%CI)
Hemisphere [†]						
Northern	Ref	Ref	Ref	Ref	Ref	Ref
Southern	15.63 (4.63–52.71)*	47.58 (10.31–219.56)*	0.89 (0.70–1.14)	0.30 (0.081–2.0)	28.99 (4.12–203.99)*	15.39 (2.81– 84.11)*
Climate zone [‡]						
Temperate	Ref	Ref	Ref	Ref	—	Ref
(Sub)Tropical	1.00 (0.47–2.15)	2.46 (1.16–5.20)*	0.91 (0.73–1.12)	0.36 (0.11–1.22)	—	2.64 (1.01– 7.63)*
Contact stringency [#]	3.97 (1.96–8.04)*	3.14 (1.83–5.38)*	0.88 (0.80–0.97)*	0.36 (0.22–0.59)*	4.05 (1.63–10.05)*	3.19 (1.66– 6.13)*
Population density ^{&}	1.88 (1.12–3.17)*	0.86 (0.55–1.34)	0.94 (0.84–1.04)	0.78 (0.41–1.49)	3.89 (1.98–7.64)*	—
1st wave Intensity	0.45 (0.28–0.73)*	0.71 (0.46–1.11)	0.97 (0.87–1.09)	1.64 (0.88–3.03)	0.36 (0.20–0.63)*	—
1st wave out-of-season onset [§]	0.50 (0.20–1.09)**	0.71 (0.46–1.11)	1.05 (0.83–1.33)	0.61 (0.15–2.48)	0.48 (0.17–1.41)	—

[†] Countries in the Northern and Southern hemisphere as defined by the World Health Organisation (WHO)

[‡] Countries in the temperate, subtropical, and tropical climate zone per Köppen and Geiger classification

[#] Contact stringency index from the Oxford Coronavirus Government Response Tracker (OxCGRT)

[&] Population density per United Nations projections measured as the number of people per square kilometers of land area in 2020

[¶] Population median age per United Nations projections in 2020 in each country

* Statistical significance is set at $p < 0.05$ (or $^{**}p < 0.10$), corresponding to 95% confidence intervals (95%CI)

[§] Out-of-season refers to RSV onset being more than 2 months out of sync compared to pre-COVID-19 mean onset timing

influence the timing of post-COVID-19 suppression RSV epidemics, which could be useful for anticipating future RSV patterns to inform planning of RSV prevention.

The comparison of epidemic characteristics between the first, second, and third waves of RSV and the pre-pandemic data suggest that RSV patterns have generally returned to typical seasonality. While prior studies have described the initial rebound of RSV following the COVID-19 pandemic [21], it remained uncertain how long it could take to return to normal pre-pandemic seasonal patterns of RSV activity. Our analyses revealed distinct patterns of RSV epidemic characteristics related to timing and/or intensity. There is ongoing interest in the dynamics of RSV during the post-COVID-19 era in different parts of the world [38]; the analyses presented here are updated regularly on an interactive dashboard [39].

Estimated earlier onset and peak timings of post-pandemic RSV waves in the Southern versus Northern hemisphere may likely reflect a higher susceptibility build-up in the Southern hemisphere due to longer time since the last RSV epidemic during pre-COVID-19 period. The association between higher population density and earlier onset of RSV during second wave suggests that

countries with more frequent human contacts, due to higher population density, were more likely to experience earlier epidemic starts, consistent with what would be expected based on social mixing patterns and the spread of respiratory pathogens [4, 40, 41].

Interestingly, contact stringency was not associated with the growth rate or intensity during the first wave of RSV following COVID-19 suppression; however, the contact stringency index remained substantially higher (>50% in most countries) and was less variable among countries during this period (Figure S5, Figure S6). However, the substantial reduction and more variability in contact stringency in some countries led to increased RSV growth rate and intensity during the second wave, as shown by our model.

Our model estimated an association between delay of the second wave of RSV and intensity of the first wave. This could be a result of depletion of susceptible individuals and/or generation of sufficient population protective immunity during the first wave [19, 42]. On the other hand, tropical/subtropical countries showed lower intensity during the first wave of RSV, which may have

resulted in earlier peaks for the second wave due to availability of enough susceptibles.

Our study had some limitations. Data on the number or percentage of individuals tested for RSV were not available; thus, we could not assess testing or reporting biases in different countries, which may explain some unexpected dynamics in the time series data, e.g. Peru, Mexico, Colombia. Increased testing for RSV following the onset of the COVID-19 pandemic has been noted as issue in interpreting surveillance data [43]. To minimise case reporting biases and changes in testing patterns over time, we examined the rate of change of the log-transformed smoothed case counts to represent the relative speed of case accumulation in order to estimate the onset, peak timing, growth rate and intensity for individual epidemic waves [35]. Of the 103 countries included in the WHO Flu Net database, 52 countries had an average of <100 annual cases during the pre-pandemic period, and another 23 countries had no data in some post-pandemic years, leaving only 28 countries for our analysis. While this criterion was necessary for model fit convergence, it could create a bias by excluding countries that had regular epidemics in the pre-pandemic era and post-pandemic patterns that did not return to “normal”.

We combined subtropical and tropical climate zone countries due to the small number of available countries in each category. Likewise, we could not perform analyses stratified by WHO regions due to insufficient data from the African and Asian regions. However, available data from other regions such as Europe and Americas were relatively large enough and of good quality. Testing data obtained from WHO platforms may change with time following data cleaning, and our results should be interpreted in the context of the data version at the time of analysis, which are also available in the Github at <https://github.com/weinbergerlab/rsv.rebound.normal.seasonality.global/tree/main/data>.

Conclusion

In conclusion, patterns of RSV activity have nearly returned to normal following COVID-19-related suppression. Timing of onset and peak of future RSV patterns need close monitoring to inform the delivery of preventive and control healthcare services.

Abbreviations

AIC	Akaike Information Criterion
CI	Confidence Interval
COVID-19	Coronavirus Disease caused by SARS-CoV-2 virus
DTW	Dynamic Time Warping
GAM	Generalised Additive Model
LCM	Local Cost Matrix
NPI	Non-Pharmaceutical Interventions
P-Spline	Penalised Spline
RSV	Respiratory Syncytial Virus
US	United States
WHO	World Health Organisation

Supplementary Information

The online version contains supplementary material available at <https://doi.org/10.1186/s12879-024-09509-4>.

Supplementary Material 1

Acknowledgements

Research reported in manuscript was fully supported by the National Institutes of Health. The content is solely the responsibility of the authors and does not necessarily represent the official views of the National Institutes of Health. We would like to thank Associate Professor Dr Joshua Warren of the Department of Biostatistics at Yale School of Public Health, Yale University for the insightful discussion on the use of P-splines in our analysis.

Author contributions

Conceptualization; DMW, VEPData curation; DTFormal analysis; DT, DMW; Funding acquisition; DMW, VEPInvestigation; DT, DMW; Methodology; DT, DMW, VEPProject administration; DMW, VEPResources; DMW, VEPSoftware; DT; Supervision; DMW; Validation; DT, DMW; Visualization; DT, DMW; Writing - original draft; DT; Writing - review & editing; DT, KL, DCW, ZZ, VEP, DMW.

Funding

This work was supported by a grant from the National Institutes of Health (R01AI137093). The content is solely the responsibility of the authors and does not necessarily represent the official views of the National Institutes of Health. The funder had no role in conceptualization, design, data collection, analysis, decision to publish, or preparation of the manuscript.

Data availability

The datasets generated and/or analysed during the current study are available in the DT's repository (<https://github.com/weinbergerlab/rsv.rebound.normal.seasonality.global/tree/main/data>).

Declarations

Ethics approval and consent to participate

These analyses used publicly available aggregate time series data at the country level and thus did not contain any data on individual human subjects. These analyses followed the guidance for the Conduct and Reporting of Modeling and Simulation Studies in the Context of Health Technology Assessment [44].

Consent for publication

Not applicable.

Competing interests

DMW has been principal investigator on grants from Pfizer and Merck to Yale University for work unrelated to this manuscript and has received consulting and/or speaking fees from Pfizer, Merck, and GSK/Affinivax. The other authors declare no competing interests.

Received: 24 February 2024 / Accepted: 13 June 2024

Published online: 25 June 2024

References

- Li Y, Wang X, Blau DM, Caballero MT, Feikin DR, Gill CJ, et al. Global, regional, and national disease burden estimates of acute lower respiratory infections due to respiratory syncytial virus in children younger than 5 years in 2019: a systematic analysis. *Lancet*. 2022;399:2047–64.
- Blau DM, Baillie VL, Els T, Mahtab S, Mutevedzi P, Keita AM et al. Deaths Attributed to Respiratory Syncytial Virus in Young Children in High-Mortality Rate Settings: Report from Child Health and Mortality Prevention Surveillance (CHAMPS). *Clinical Infectious Diseases*. 2021;73 Supplement_3:S218–28.
- Shi T, Denouel A, Tietjen AK, Campbell I, Moran E, Li X, et al. Global Disease Burden estimates of respiratory Syncytial Virus–Associated Acute respiratory infection in older adults in 2015: a systematic review and Meta-analysis. *J Infect Dis*. 2020;222 Supplement7:S577–83.

4. Pitzer VE, Viboud C, Alonso WJ, Wilcox T, Metcalf CJ, Steiner CA, et al. Environmental drivers of the Spatiotemporal Dynamics of Respiratory Syncytial Virus in the United States. *PLoS Pathog*. 2015;11:e1004591.
5. Obando-Pacheco P, Justicia-Grande AJ, Rivero-Calle I, Rodríguez-Tenreiro C, Sly P, Ramilo O, et al. Respiratory Syncytial Virus Seasonality: A Global Overview. *J Infect Dis*. 2018;217:1356–64.
6. Hamid S. Seasonality of respiratory Syncytial Virus — United States, 2017–2023. *MMWR Morb Mortal Wkly Rep*. 2023;72.
7. Chadha M, Hirve S, Bancej C, Barr I, Baumeister E, Caetano B, et al. Human respiratory syncytial virus and influenza seasonality patterns—early findings from the WHO global respiratory syncytial virus surveillance. *Influenza Other Respir Viruses*. 2020;14:638–46.
8. Chow EJ, Uyeki TM, Chu HY. The effects of the COVID-19 pandemic on community respiratory virus activity. *Nat Rev Microbiol*. 2022. <https://doi.org/10.1038/s41579-022-00807-9>.
9. Tempia S, Walaza S, Bhiman JN, McMorrow ML, Moyes J, Mkhencele T, et al. Decline of influenza and respiratory syncytial virus detection in facility-based surveillance during the COVID-19 pandemic, South Africa, January to October 2020. *Eurosurveillance*. 2021;26:2001600.
10. Lumley SF, Richens N, Lees E, Cregan J, Kalimeris E, Oakley S, et al. Changes in paediatric respiratory infections at a UK teaching hospital 2016–2021; impact of the SARS-CoV-2 pandemic. *J Infect*. 2022;84:40–7.
11. Opek MW, Yeshayahu Y, Glatman-Freedman A, Kaufman Z, Sorek N, Brosh-Nissimov T. Delayed respiratory syncytial virus epidemic in children after relaxation of COVID-19 physical distancing measures, Ashdod, Israel, 2021. *Eurosurveillance*. 2021;26:2100706.
12. Agha R, Avner JR. Delayed seasonal RSV surge observed during the COVID-19 pandemic. *Pediatrics*. 2021;148:e2021052089.
13. Casalegno J-S, Ploin D, Cantais A, Masson E, Bard E, Valette M, et al. Characteristics of the delayed respiratory syncytial virus epidemic, 2020/2021, Rhône Loire, France. *Eurosurveillance*. 2021;26:2100630.
14. Billard M, van de Ven PM, Baraldi B, Kragten-Tabatabaie L, Bont LJ, Wildenbeest JG. International changes in respiratory syncytial virus (RSV) epidemiology during the COVID-19 pandemic: Association with school closures. *Influenza Other Respir Viruses*. 2022;16:926–36.
15. Koltai M, Krauer F, Hodgson D, van Leeuwen E, Treskova-Schwarzbach M, Jit M, et al. Determinants of RSV epidemiology following suppression through pandemic contact restrictions. *Epidemics*. 2022;40:100614.
16. Hale T, Angrist N, Goldszmidt R, Kira B, Petherick A, Phillips T, et al. A global panel database of pandemic policies (Oxford COVID-19 Government Response Tracker). *Nat Hum Behav*. 2021;5:529–38.
17. Eden J-S, Sikazwe C, Xie R, Deng Y-M, Sullivan SG, Michie A, et al. Off-season RSV epidemics in Australia after easing of COVID-19 restrictions. *Nat Commun*. 2022;13:2884.
18. Zheng Z, Warren JL, Artin I, Pitzer VE, Weinberger DM. Relative timing of respiratory syncytial virus epidemics in summer 2021 across the United States was similar to a typical winter season. *Influenza Other Respir Viruses*. 2022;16:617–20.
19. Zheng Z, Pitzer VE, Shapiro ED, Bont LJ, Weinberger DM. Estimation of the timing and intensity of reemergence of respiratory Syncytial Virus following the COVID-19 pandemic in the US. *JAMA Netw Open*. 2021;4:e2141779.
20. McNab S, Ha Do LA, Clifford V, Crawford NW, Daley A, Mulholland K, et al. Changing epidemiology of respiratory Syncytial Virus in Australia—delayed re-emergence in Victoria compared to Western Australia/New South Wales (WA/NSW) after prolonged lock-down for Coronavirus Disease 2019 (COVID-19). *Clin Infect Dis*. 2021;73:2365–6.
21. Li Y, Wang X, Cong B, Deng S, Feikin DR, Nair H. Understanding the potential drivers for respiratory Syncytial Virus Rebound during the Coronavirus Disease 2019 Pandemic. *J Infect Dis*. 2022;225:957–64.
22. Baker RE, Park SW, Yang W, Vecchi GA, Metcalf CJE, Grenfell BT. The impact of COVID-19 nonpharmaceutical interventions on the future dynamics of endemic infections. *Proceedings of the National Academy of Sciences*. 2020;117:30547–53.
23. World Health Organization. Global Influenza Programme, FluNet Data. 2023.
24. NOAA. US National Oceanic Atmospheric Administration on Climate Zones. 2023. <https://www.noaa.gov/jetstream/global/climate-zones/jetstream-max-addition-k-ppen-geiger-climate-subdivisions>. Accessed 6 Jul 2023.
25. Hastie T, Tibshirani R. Generalized additive models. *Stat Sci*. 1986;1:297–310.
26. Wood S. mgcv: Mixed GAM Computation Vehicle with Automatic Smoothness Estimation. 2023.
27. Artin B. pspline.inference: estimation of characteristics of Seasonal and sporadic infectious disease outbreaks using generalized additive modeling with penalized basis splines. 2021.
28. Aghabozorgi S, Seyed Shirshorshidi A, Ying Wah T. Time-series clustering – A decade review. *Inform Syst*. 2015;53:16–38.
29. Giorgino T. Computing and visualizing dynamic time warping alignments in R: the Dtw Package. *J Stat Softw*. 2009;31:1–24.
30. Sardá-Espinosa A. Time-Series Clustering in R using the Dtwclust Package. *R J*. 2019;11:22.
31. Ratanamahatana C, Keogh EJ. Everything you know about Dynamic Time Warping is Wrong. 2004.
32. Ratanamahatana CA, Keogh E. Making Time-series Classification More Accurate Using Learned Constraints. In: *Proceedings of the 2004 SIAM International Conference on Data Mining (SDM)*. Society for Industrial and Applied Mathematics; 2004. pp. 11–22.
33. Dau HA, Silva DF, Petitjean F, Forestier G, Bagnall A, Mueen A, et al. Optimizing dynamic time warping's window width for time series data mining applications. *Data Min Knowl Disc*. 2018;32:1074–120.
34. Hastie T, Tibshirani R, Friedman J. *The elements of statistical learning*. New York, NY: Springer; 2009.
35. Parag KV, Thompson RN, Donnelly CA. Are Epidemic Growth Rates more informative than Reproduction numbers? *J Royal Stat Soc Ser A: Stat Soc*. 2022;185 Supplement1:55–15.
36. Stone M. An asymptotic equivalence of choice of Model by Cross-validation and Akaike's Criterion. *J Royal Stat Soc Ser B (Methodological)*. 1977;39:44–7.
37. Sauerbrei W, Perperoglou A, Schmid M, Abrahamowicz M, Becher H, Binder H, et al. State of the art in selection of variables and functional forms in multi-variable analysis—outstanding issues. *Diagn Prognostic Res*. 2020;4:3.
38. Billard M-N, Bont LJ. Quantifying the RSV immunity debt following COVID-19: a public health matter. *Lancet Infect Dis*. 2023;23:3–5.
39. Weinberger Lab. Understanding the patterns of global re-emergence of RSV following COVID-19 pandemic. 2023. <https://rsvglobalreport.github.io/dashboard/posts/dashboard/>. Accessed 21 Jun 2023.
40. Keeling MJ, Rohani P. *Modeling infectious diseases in humans and animals*. Princeton University Press; 2011.
41. Zheng Z, Pitzer VE, Warren JL, Weinberger DM. Community factors associated with local epidemic timing of respiratory syncytial virus: a spatiotemporal modeling study. *Sci Adv*. 2021. <https://doi.org/10.1126/sciadv.abd6421>.
42. White LJ, Mandl JN, Gomes MGM, Bodley-Tickell AT, Cane PA, Perez-Brena P, et al. Understanding the transmission dynamics of respiratory syncytial virus using multiple time series and nested models. *Math Biosci*. 2007;209:222–39.
43. Petros BA, Milliren CE, Sabeti PC, Ozonoff A. Increased Pediatric Respiratory Syncytial Virus Case counts following the emergence of severe Acute Respiratory Syndrome Coronavirus 2 can be attributed to changes in testing. *Clin Infect Dis*. 2024;ciae140.
44. Dahabreh IJ, Trikalinos TA, Balk EM, Wong JB. Recommendations for the Conduct and Reporting of modeling and Simulation studies in Health Technology Assessment. *Ann Intern Med*. 2016;165:575–81.
45. JGraph. Draw.io. Draw, a configurable diagramming or whiteboarding visualization application. 2023.

Publisher's Note

Springer Nature remains neutral with regard to jurisdictional claims in published maps and institutional affiliations.